

Active Contour based Medical Image Segmentation



by

Uragoda Appuhamilage Aruni Niroshika

**Thesis submitted to the University of Sri Jayewardenepura for the award
of the Degree of Doctor of Philosophy in Computer Science on 2014**

Certification of Supervisors

We certify that the candidate has incorporated all corrections, additions, and amendments recommended by the examiners.



Prof. R.G.N. Meegama

16/03/2015

Prof. R. G. N. MEEGAMA
Department of Computer Science
Faculty of Applied Sciences
University of Sri Jayawardene
Nugegoda - Sri Lanka.



Dr. Mahesha Kapurubandara

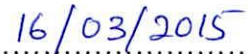
Dr. Mahesha Kapurubandara
Dean International
Sri Lanka Institute of Information Technology

DECLARATION

The work described in this thesis was carried out by me under the supervision of Prof. R.G.N. Meegama, Department of Computer Science, Faculty of Applied Sciences, University of Sri Jayewardenepura and Dr. Mahesha Kapurubandara, Department of Information Technology, Faculty of Computing, Sri Lanka Institute of Information Technology, and a report on this has not been submitted in whole or in part to any university or any other institution for any other Degree.



.....
Uragoda Appuhamilage Aruni Niroshika




.....
Date

We certify that the above statement made by the candidate is true and that this thesis is suitable for submission to the University for the purpose of evaluation.



.....
Prof. R.G.N. Meegama



Prof. R. G. N. MEEGAMA
Department of Computer Science
Faculty of Applied Sciences
University of Sri Jayawardenepura
Nugegoda - Sri Lanka.



.....
Dr. Mahesha Kapurubandara

Dr. Mahesha Kapurubandara
Dean International
Sri Lanka Institute of Information Technology

Table of Contents

LIST OF TABLES	iv
LIST OF FIGURES	vi
LIST OF ALGORITHMS	ix
LIST OF ABBREVIATIONS	x
ACKNOWLEDGEMENTS	xi
ABSTRACT	xiii
CHAPTER 1	1
INTRODUCTION	1
1.1 Research Problem	8
1.1.1 Distance Between Adjacent Snaxel Points	8
1.1.2 Behavior of the Elasticity Force	8
1.1.3 Detection of False Corner Points and Intensity Extremes	9
1.1.3.1 Detection of False Corner Points	10
1.1.3.2 Detection of False Intensity Extremes	10
1.2 Objectives	11
1.3 Organization of the Report	23
CHAPTER 2	15
LITERATURE SURVEY	15
2.1 Active Contour Models	15
2.2 Corner Detection Operators	19
CHAPTER 3	22
METHODOLOGY: THE BLAID OPERATOR	22
3.1 Corner Detection	22

3.1.1	The Harris Operator	22
3.2	The BLAID Operator	26
CHAPTER 4		34
METHODOLOGY: THE PROPOSED SNAKE MODEL WITH THE BLAID OPERATOR		34
4.1	Active Contour Model	34
4.2	The Active Contour Model with BLAID Operator	39
CHAPTER 5		46
RESULTS AND DISCUSSION		46
5.1	The Test Results: BLAID Operator	47
5.1.1	Experiments with Synthetic Images	47
5.1.1.1	Accuracy	48
5.1.1.2	Affine Invariancy	50
5.1.1.3	Localization	54
5.1.1.4	Sensitivity to Noise	56
5.1.2	Experiments with a Real Image	58
5.1.3	Discussion	60
5.2	The Test Results: Snake Model with BLAID Operator	61
5.2.1	Experiments with Synthetic Images	63
5.2.2	Experiments with Real Images	67
5.2.2.1	Experiments with X-ray Bone Images	68
5.2.2.2	Experiments with Dental X-ray Images	71
5.2.3	Computational Complexity	76
5.2.4	Computational Speed	77
5.2.5	Discussion	78

CHAPTER 6	81
CONCLUSIONS	81
6.1 Conclusions	81
6.1.1 Corner Detection	82
6.1.2 Snake Model	85
6.2 Possibilities of Other Applications	90
6.2.1 Surface Wrapping	90
6.2.1.1 Change the Surface Topology	91
6.2.1.2 Change the Mesh Structure	92
6.2.2 Application on 3D Volumetric Data	94
6.2.3 Possibilities of Other Applications	95
6.2.4 Increasing the Window Size of the BLAID Operator	96
REFERENCES	98
APPENDIX 1	117
List of Publications and Communications	117
APPENDIX 1I	119
Mathematical Derivations	119

LIST OF TABLES

Table 5.1 Comparison of measurements for different operators applied on the image in Fig. 5.1.	49
Table 5.2 Consistency of Corner Numbers (CNN) obtained by the BLAID operator under different transformations.	52
Table 5.3: Consistency of Corner Numbers (CNN) obtained by four different operators under different transformations	53
Table 5.4 Comparison of Localization Errors (L_e) for different operators applied on different images.	55
Table 5.5 Comparison of errors (e) for different operators applied on the image in Fig. 5.4.	57
Table 5.6 Errors (e) obtained by the proposed BLAID operator under different SNR values.	58
Table 5.7 Comparison of measurements for different operators applied on the image in Fig. 5.5.	59
Table 5.8 Comparison of Average Distance Errors (e) for different snake models applied to images in Fig. 5.7.	65
Table 5.9 Comparison of average distance errors (e) for different snake models applied on the image in Fig. 5.8.	66
Table 5.10 Average distance errors obtained by the proposed snake model under different SNR values on image in Fig. 5.8.	67
Table 5.11 Comparison of average distance errors (e) for different snake models applied on the image in Fig. 5.9 (bone fracture of the arm).	68

Table 5.12 Average Distance Errors (e) for different snake models applied to images in Fig. 5.10.	70
Table 5.13 Average Distance Errors (e) for different snake models applied to images in Fig. 5.11.	73
Table 5.14 Tukey's simultaneous tests applied on different snake models to compare the performance of the proposed model.	75
Table 5.15 Comparison of mean values of average distance errors between the snake models.	75
Table 5.16. Execution time comparison (for 200 iterations)	77

LIST OF FIGURES

- Fig. 1.1 The elasticity force $F_{elasticity}$ drags the snaxel point more into the object even near the sharp corner. 9
- Fig. 1.2 False feature points: (a) an isolated point, (b) a thin line ending and (c) a high curvature curve bend. 10
- Fig. 3.1 Circular Array Illustrations: (a) A possible corner region and its corresponding circular array of size 4 where each and every element has at least one adjacent neighbor and (b) Uninterested region and its corresponding circular array of size 3 with a disjointed element without any adjacent neighbors. Edges of the adjacent points within one pixel difference are defined in dotted lines. 29
- Fig. 3.2 Local image structures of possible corner patterns within 3×3 window ((a) - (d)). The center pixel $\mathbf{P}_{(x,y)}$ is denoted using a filled circle, neighboring pixels within the set S are in empty circles, possible edge connections are in dotted lines and corner regions are highlighted in solid lines. 30
- Fig. 3.3 A section of a target object where $\mathbf{P}_{(x,y)}$ is the detected candidate corner point with three similar neighbours. 32
- Fig. 4.1 Position of the initial contour located around the targeted object (shaded region) 41
- Fig. 4.2 Re-parameterization step of the deforming snake, where the curve segment is pushed towards a sharp corner: (a) an instance where $d < T_d$ and (b) corner point \mathbf{C}_i is added between \mathbf{V}_i and \mathbf{V}_{i+1} and the curve segment is pushed towards the corner. 43
- Fig. 4.3 Re-parameterization step of the deforming snake, where the curve segment is pulled backwards to the corner point: (a) and instance where $d < T_d$ and (b) corner point \mathbf{C}_j is added between \mathbf{V}_{i+1} and \mathbf{V}_{i+2} and the curve segment is pulled back to the corner. 43

- Fig. 5.1 Illustrations of corner detection on a synthetic image. (a) The Reference Image (b) Harris, (c) SUSAN, (d) FAST, (e) SURF and (f) BLAID operator. 48
- Fig. 5.2 Illustrations of corner detection on transformed images. (a) Original Image (b) Rotated - 30°, (c) Rotated - 60°, (d) Rotated - 90°, (e) Zoomed In, (f) Zoomed out, (g) non-uniform vertically scaled and (h) non-uniform horizontally scaled. 50
- Fig. 5.3: Illustrations of corner detection on transformed images. (first row) Harris operator, (second row), SUSAN operator, (third row) FAST operator, (fourth row) SURF operator 53
- Fig. 5.4 Illustrations of the five different corner detection operators on synthetic images with added Gaussian noise: (a) The test image, (b)Harris, (c) SUSAN, (d) FAST, (e) SURF and (f) BLAID. 56
- Fig. 5.5 Illustrations of corner detection on a real image. (a) The Reference Image, (b) Harris, (c) SUSAN, (d) FAST, (e) SURF and (f) BLAID. 59
- Fig. 5.6 Deformation of the proposed snake model towards the boundary of a foreground object in a synthetic image: (a) corner points defined by the BLAID operator, (b) initial contour defined by the operator, (c) to (k) intermediates taken after each 30 iterations and (l) final position after 300 iterations. 63
- Fig. 5.7 Convergence of the five different snake models on three different synthetic images: (first column) Kass Snake, (second column) Balloon Snake, (third column) GVF Snake, (fourth column) NURBS Snake, and (fifth column): Proposed Snake Model 64
- Fig. 5.8 Convergence of the five different snake models on synthetic images with added Gaussian noise: (a) Kass snake, (b) Balloon snake, (c) GVF snake, (d) NURBS snake and (e) proposed snake model. 66

- Fig. 5.9 Illustrations of convergence of a linear fracture of the arm bone with: (a) Kass snake, (b) balloon snake, (c) GVF snake, (d) NURBS snake and (e) proposed snake model. 68
- Fig. 5.10 Illustrations of proposed snake model converging: (a) pathological fracture on right humerus due to bone cyst, (b) broken collar bone, (c) linear fracture of bone and (d) a fractures of the greater trochanter. 70
- Fig. 5.11 (top image): dental X-ray image of teeth and (bottom two rows): convergence of the proposed snake on each tooth. 72
- Fig. 6.1 Illustrations of surface wrapping: (a) Projection of surface wrapping, where a surface is wrapping around a 3D sphere, (b) plastic material is wrapped around the 3D object – in Blender. 90
- Fig. 6.2 This localized re-meshing of the facet F_i : (a) facet F_i is pushed towards a sharp corner C_j , (b) The facet F_i is locally re-meshed by performing 1-to-3 splitting from C_j . 93
- Fig. 6.3 From (a) - (d): Local image structures of possible corner patterns within 5×5 window. The center pixel $P_{(x,y)}$ is denoted using a filled circle, possible edge connections are highlighted in dotted lines. 97

LIST OF ALGORITHMS

Algorithm 3.1	: Pseudo code of Harris Operator	25
Algorithm 3.2	: BLAID Operator	32
Algorithm 4.1	: Initialization, Deformation and Re-parameterization	44

LIST OF ABBREVIATIONS

MRI	Magnetic Resonance Imaging
CT	Computer Tomography
CAD	Computer-Aided Diagnosis
BLAID	Boundaries from Locally Adaptive Isotropic Detection
ACID	Affine Cell Decomposition
GVF	Gradient Vector Flow
NURBS	Non-Uniform Rational B-Spline
D-NURBS	Dynamic Non-Uniform Rational B-Spline
SSD	Sum of Squared Difference
SUSAN	Smallest Uni-value Segment with an Assimilating Nucleus
FAST	Feature from Accelerated Segment Test
SURF	Speeded Up Robust Features
ROI	Region of Interest
CCN	Consistency of Corner Numbers
SNR	Signal to Noise Ratio

ACKNOWLEDGEMENTS

Apart from my effort, this research is an outcome of proper guidance, encouragement, and well wishes of many others. I take this opportunity to express my gratitude for all of them who have been involved in the successful completion of this research study.

I must offer my profoundest gratitude to my supervisor, Prof. R.G.N. Meegama, for his patience, motivation, thoughtful guidance, and immense knowledge. Without his proper guidance, this research would not have been possible.

Besides my supervisor, I thank to Dr. Mahesha Kapurubandara, the co-supervisor, for her encouragements and comments. Further, I extend my profound thanks to other professionals who contributed towards this research, namely; Dr. R.S. Lokupitiya, and Dr. D.K.S. Kannangara.

Secondly, I would like to express my gratitude to the key person who has been behind every milestone in my life, my loving husband Gayan. Many thanks for encouraging me, being with me during this hard time, and tolerating my stress at his level best.

I thank Ms. Antoinette Hettiaratchy, for her friendly assistance with the paperwork, proof reading of many of my articles and the thesis. I am also deeply thankful to Prof. Lalith Gamage, MD/CEO, Sri Lanka Institute of Information Technology and Mr. Nuwan Kodagoda, Head/IT for making it possible for me to study during my work by providing adequate time and resources. I wish to thank Ms. Sachintha Ranathunga of the Faculty of Graduate Studies, University of Sri Jayewardenepura, for her kind cooperation throughout the duration of the research.

Finally, I must of course thank few persons for their encouragement and friendship, namely; Prof. George Mann, Mohan Liyanage, Dr. Tharangie, Mr. Ranjit Jayaweera Bandara, Ian Karunaratna, Heshani Kularatna, and Aith Perera.

Active Contour based Medical Image Segmentation

by Uragoda Appuhamilage Aruni Niroshika

ABSTRACT

The main contribution of this research study is to devise an effective active contour model to segment discontinuous boundaries in X-ray Images. This involves the improvement of the active contour's capability in detecting sharp corners by incorporating prior knowledge about the significant corners of the object of interest, while preserving the general energy terms.

Active contours are a form of curves that deform according to an energy minimising function and are widely used in computer vision and image processing applications. In this research study, a new technique of active contour model to extract boundaries of objects having sharp corners is devised. By incorporating a priori knowledge of significant corners of the object into the deforming contour, the proposed active contour is able to deform towards the boundaries of the object without surpassing the corners.

Moreover, all the significant corner points/discontinuous regions of the targeted object should be identified accurately during the initialization step of the proposed snake model. In order to perform this task with less user involvement, a competent corner detection operator should be integrated with the proposed snake model. Therefore a novel corner detection operator known as BLAID (Boundaries from Locally Adaptive Isotropic

Detection), which is capable of detecting corner points that exist only on the boundary of an object, is integrated with the proposed snake model.

The ability of the new technique to accurately extract features of interest of anatomical structures in medical X-ray images having sharp corners is tested. The proposed model demonstrated significantly better results on detecting corners comparatively with the other existing models. We demonstrated the efficiency of our snake model by testing it on images with additive Gaussian noise. The experimental results demonstrate that the proposed snake model performs well for the images having an SNR of > 20 .